Lysophosphatidic acid triggers mast cell-driven atherosclerotic plaque destabilization by increasing vascular inflammation.

Bot, M.; Jager, S.C.; MacAleese, L.; Lagraauw, H.M.; Berkel, T.J.C. van; Quax, P.H.A.; ... ; Bot, I.

Lysophosphatidic acid triggers mast cell-driven atherosclerotic plaque destabilization by increasing vascular inflammation[S]

Martine Bot,[1,*] Saskia C. A. de Jager,[1,*] Luke MacAleese,[†] H. Maxime Lagraauw,[*] Theo J. C. van Berkel,[*] Paul H. A. Quax,[§,] Johan Kuiper,[*] Ron M. A. Heeren,[†] Erik A. L. Biessen,[††] and Ilze Bot[2,*,†,**]**

Division of Biopharmaceutics,* Leiden Academic Centre for Drug Research, 2333 CC, Leiden University, Leiden, The Netherlands; FOM-AMOLF,[†] 1098 XG Amsterdam, The Netherlands; Einthoven Laboratory for Experimental Vascular Medicine[§] and Department of Surgery,** Leiden University Medical Center, 2300 RC, Leiden, The Netherlands; and Experimental Vascular Pathology Group, Department of Pathology,[††] Maastricht University Medical Center, 6202 AZ, Maastricht, The Netherlands

Abstract Lysophosphatidic acid (LPA), a bioactive lysophospholipid, accumulates in the atherosclerotic plaque. It has the capacity to activate mast cells, which potentially exacerbates plaque progression. In this study, we thus aimed to investigate whether LPA contributes to plaque destabilization by modulating mast cell function. We here show by an imaging mass spectrometry approach that several LPA species are present in atherosclerotic plaques. Subsequently, we demonstrate that LPA is a potent mast cell activator which, unlike other triggers, favors release of tryptase. Local perivascular administration of LPA to an atherosclerotic carotid artery segment increases the activation status of perivascular mast cells and promotes intraplaque hemorrhage and macrophage recruitment without impacting plaque cell apoptosis. The mast cell stabilizer cromolyn could prevent intraplaque hemorrhage elicited by LPA-mediated mast cell activation. Finally, the involvement of mast cells in these events was further emphasized by the lack of effect of perivascular LPA administration in mast cell deficient animals. We demonstrate that increased accumulation of LPA in plaques induces perivascular mast cell activation and in this way contributes to plaque destabilization in vivo. This study points to local LPA availability as an important factor in atherosclerotic plaque stability.—Bot, M., S. C. A. de Jager, L. MacAleese, H. M. Lagraauw, T. J. C. van Berkel, P. H. A. Quax, J. Kuiper, R. M. A. Heeren, E. A. L. Biessen, and I. Bot. **Lysophosphatidic acid triggers mast cell-driven atherosclerotic plaque destabilization by increasing vascular inflammation. *J. Lipid Res.* 2013.** 54: **1265–1274.**

Supplementary key words atherosclerosis • plaque stability • macrophage

Atherosclerotic plaque rupture is a leading cause of acute coronary syndromes, such as unstable angina and myocardial infarction (1). Inflammatory cells are regarded as key players in the pathogenesis of plaque rupture (2, 3), and the mast cell, a potent inflammatory cell, has been shown to accumulate in the rupture-prone shoulder region of human atheromas (4). Activated mast cells have been identified in the adventitia of vulnerable and ruptured lesions in patients with myocardial infarction, and more importantly, their numbers and degree of activation were found to correlate with the incidence of plaque rupture and erosion (5). We previously demonstrated that systemic mast cell activation during atherogenesis leads to increased plaque progression in apoE deficient mice (6), while others show that the absence of mast cells, and in particular mast cell-derived interleukin (IL)-6 and interferon (IFN)-γ, attenuated atherosclerotic lesion development in low-density lipoprotein receptor-deficient ($LDLr^{-/-}$) mice (7). Moreover, focal activation of mast cells in the adventitia of advanced carotid artery plaques promoted macrophage apoptosis, microvascular leakage, de novo leukocyte influx, and the incidence of intraplaque hemorrhage. Mast cell stabilization by cromolyn was seen to prevent these pathophysiological events (6).

Various pathways of mast cell activation have been demonstrated such as cross-linking of the high-affinity

This study was supported by grant TSN2004.001 from the Netherlands Thrombosis Foundation (M.B.), grant 916.86.046 from the Netherlands Organization for Scientific Research (I.B.), and grant 2003T201 from the Netherlands Heart Foundation (E.A.L.B.). The authors report no conflicts of interest.

Manuscript received 3 October 2012 and in revised form 29 January 2013.

Published, JLR Papers in Press, February 10, 2013
DOI 10.1194/jlr.M032862

Abbreviations: $apoE^{-/-}$, apolipoprotein E-deficient; BMMC, bone marrow-derived mast cell; IL, interleukin; $LDLr^{-/-}$, low density lipoprotein receptor-deficient; LPA, lysophosphatidic acid; MCP, monocyte chemoattractant protein; MOMA-2, monocyte/macrophage antibody-2; oxLDL, oxidized low density lipoprotein; PMC, peritoneal mast cell; SIMS, secondary ion mass spectrometry; TOF, time-of-flight; TUNEL, terminal deoxytransferase dUTP nick-end labeling.

[1] M. Bot and S. C. A. de Jager contributed equally to this work.
[2] To whom correspondence should be addressed.
e-mail: i.bot@lacdr.leidenuniv.nl

[S] The online version of this article (available at http://www.jlr.org) contains supplementary data in the form of four figures.

IgE receptor by multiple IgE molecules (8), neurogenic stimulation (8, 9), inflammatory stimuli (e.g., tumor necrosis factor α and IL-1), and complement factors (e.g., C3a and C5a) (10). Although the endogenous triggers for mast cell activation in atherosclerosis are still unknown, IgE (11), IgG-oxidized low-density lipoprotein (oxLDL) immune complexes (12), the neuropeptide substance P (9, 13), and the complement system (14) were suggested to activate mast cells in atherosclerosis. Furthermore, oxLDL itself was seen to promote mast cell activation (15, 16). Lysophosphatidic acid (LPA), a bioactive lipid and major constituent of modified LDL, may be a potential candidate in this regard, as mast cells express several LPA receptors (17) through which LPA can affect mast cell function. Indeed, Bagga et al. demonstrated that LPA accelerates human mast cell proliferation and differentiation via $LPA_{1/3}$- and peroxisome proliferator-activated receptor γ-dependent pathways (18). In addition, LPA triggers the release of a wide range of proinflammatory chemokines such as macrophage inflammatory protein-1β, IL-8, eotaxin, and monocyte chemoattractant protein (MCP)-1, which can attract inflammatory cells to the arterial wall (19). It is worth noting that LPA progressively accumulates in human and mouse atherosclerotic plaques (20, 21), and was shown to be involved in atherogenesis by virtue of its pro-coagulating capacity (20, 22) and its endothelial/leukocyte interaction (23, 24).

In this study, we have therefore investigated the potential involvement of LPA in mast cell-driven plaque destabilization. We demonstrate that LPA can activate adventitial mast cells, promote monocyte recruitment and microvascular leakage, and lead to an enhanced incidence of intraplaque hemorrhage. Finally, our data indicate that the adverse events of LPA-induced mast cell activation can be largely inhibited by the mast cell stabilizer cromolyn.

METHODS

Animals

All animal work was performed in compliance with the Dutch government guidelines and conducted in conformity with the Health Service Policy (PHS) on Humane Care and Use of Laboratory Animals. C57Bl/6 mice (Charles River, Maastricht, The Netherlands) and mast cell deficient Kit(W^{-sh}/W^{-sh}) mice (Jackson Laboratories) were maintained in the local animal breeding facility. Male $LDLr^{-/-}$ mice, apolipoprotein E-deficient ($apoE^{-/-}$) mice, and $apoE^{-/-}$Kit(W^{-sh}/W^{-sh}) mice were fed a Western-type diet containing 0.25% cholesterol and 15% cacaobutter (SDS, Sussex, UK). Atherosclerotic carotid artery lesion formation was induced by perivascular collar placement as described previously (25). Mice were anesthetized by subcutaneous injection of ketamine (60 mg/kg, Eurovet Animal Health, Bladel, The Netherlands), fentanyl citrate, and fluanisone (1.26 mg/kg and 2 mg/kg respectively, VetaPharma Ltd, Leeds, UK).

MS imaging

Lipid distribution of carotid artery plaques in $LDLr^{-/-}$ mice was determined at 9 weeks after perivascular collar placement. Hereto, mice were sacrificed by perfusion through the left cardiac ventricle with phosphate-buffered saline (150 mM NaCl, 1.5 mM NaH_2PO_4, 8.6 mM Na_2HPO_4, pH 7.4) followed by perfusion with 128 mM ammonium bicarbonate to remove salts which interfere with secondary ion mass spectrometry (SIMS) measurements. Subsequently, the common carotid arteries were both excised, embedded in 10% gelatin at 30°C and snap-frozen in liquid nitrogen for optimal lipid preservation.

Transverse 10 μm cryosections were prepared on a Leica CM 3050 cryostat (Leica Microsytems, Rijswijk, The Netherlands) at −20°C. The sections were cut in a proximal direction from the carotid bifurcation and mounted in order on a parallel series of glass slides, alternating between 1% gelatin-coated slides for immunohistological staining and conductive transparent indium tin oxide-coated slides (Delta Technologies, Stillwater, MN) for time-of-flight (TOF)-SIMS, which are stored at −80°C until further use. The sample surface of a series of sections mounted on conductive slides were sputter coated with gold using a Quorum Technologies (Newhaven, East Sussex, UK) SC7640 sputter coater.

All static SIMS experiments were performed on a Physical Electronics (Eden Prairie, MN) TRIFT-II TOF-SIMS instrument described elsewhere (26) and newly equipped with a gold liquid metal ion gun. Secondary ions were extracted through a 3.2 keV electric field into the TOF analyzer and postaccelerated by an additional 8 keV field prior to detection on a dual multichannel plate/phosphor screen detector. All experiments were performed with a primary ion beam current of 1 nA, a primary pulse length of 18 ns, and a primary ion energy of 22 keV. The ion dose was such that all analyses were conducted at or under the static SIMS threshold (10^{13} ions/cm^2) for reduced fragmentation of analytes. The instrument was calibrated in both positive and negative mode on high-occurrence elements and fragments such as $H^{+/-}$, CH_n^+, Na^+, K^+, O^-, and OH^-. To ensure correct identification of the lipid species of interest, reference samples of 18:1/18:1 PA, 18:1 LPA, and S1P were analyzed with SIMS and matrix-enhanced SIMS.

Cell culture

The capacity of LPA to activate murine mast cells was studied on MC/9 mast cells as well as on freshly isolated peritoneal mast cells (PMCs). MC/9 cells were cultured as described previously (6). Bone marrow-derived mast cells (BMMCs) were cultured by culturing bone marrow cells at a density of 0.25×10^6 cells in RPMI containing 10% fetal bovine serum (FBS), 2 mmol/l L-glutamine, 100 U/ml penicillin, 100 μg/ml streptomycin, and murine IL3 for 4 weeks. Total RNA was extracted from these cells with guanidine thiocyanate, reverse transcribed using M-MuLV reverse transcriptase (RevertAid, MBI Fermentas, Leon-Roth, Germany) and expression of target genes was measured by quantitative PCR on an ABI PRISM 7500 Taqman apparatus (Applied Biosystems, Foster City, CA).

PMCs from C57Bl/6 mice were isolated by lavage of the peritoneal cavity with 10 ml of ice-cold PBS. Cells were seeded at 2×10^6 cells/ml in RPMI containing 10% fetal bovine serum (FBS), 2 mmol/l L-glutamine, 100 U/ml penicillin, 100 μg/ml streptomycin, and murine IL3 and allowed to attach for 1 h. Nonadhered cells were seeded at 2.5×10^5 cells/ml and used for degranulation experiments. MC/9 cells, BMMCs, and PMCs (2.5×10^5 cells) were activated by incubation with compound 48/80 (0.5 μg/ml, Sigma, Zwijndrecht, The Netherlands) or 10 μg/ml LPA (22 μmol/l, 18:1, Sigma) (n = 3 per condition) for 30 min at 37°C in HEPES-tyrode supplemented with 0.1% fatty acid-free BSA (BSA, Sigma). Cells were centrifuged (1,500 rpm, 5 min) and the releasate was used for further experiments. For total (100%) release measurements, mast cells were lysed with 10% Triton X-100 and untreated control cell supernatant served as 0% release control. In vivo mast cell activation was determined in C57Bl/6 mice and mast cell deficient Kit(W^{-sh}/W^{-sh}) mice that had received intraperitoneal

injections of LPA (1.75 μg) or PBS (n = 4 per group). At baseline and at 2 h after injection, the releasate was collected by flushing the peritoneal cavity with ice-cold PBS.

β-Hexosaminidase activity was determined by adding 50 μl of releasate to 50 μl 2 mM 4-nitrophenyl *N*-acetyl-b-D-glucosaminide (Sigma) in 0.2 M citrate (pH 4.5) and incubated at 37°C for 2 h. After addition of 150 μl 1 M Tris (pH 9.0), absorbance (optical density) was measured at 405 nm (OD405). To measure chymase and tryptase release after degranulation, 50 μl supernatant was added to 2 mM S-2288 (tryptase substrate, Chromogenix, Lexington, MA) or S-2586 (chymase substrate, Chromogenix) in PBS supplemented with 100 U/ml heparin. After 2 h (tryptase) or 24 h (chymase) at 37°C, OD405 was measured. Values are expressed as percentage of total release. MCP-1 levels were determined by ELISA according to the manufacturer's protocol (eBioscience).

RAW 264.7 macrophage cells were cultured in Dulbecco's modified Eagle medium (DMEM) containing 10% FBS, 2 mmol/l L-glutamine, 100 U/ml penicillin, and 100 μg/ml streptomycin. For proliferation experiments cells were seeded in 24-well dishes at a density of 1×10^5 cells/ml in DMEM containing 1% FBS, 2 mmol/l L-glutamine, 100 U/ml penicillin, and 100 μg/ml streptomycin for 24 h to synchronize cell cycle. Subsequently, fresh serum-free DMEM containing 0.2% BSA and 18:1 LPA at various concentrations was added to the cells and cultured for 40 h without medium change. Ten percent FBS in DMEM was used as a positive control. After 16 h [^{3}H]thymidin (5.0 μCi/well; GE Healthcare, Eindhoven, The Netherlands) was added and cells were incubated further for 24 h. Thereafter, cells were washed three times with PBS, lysed with 0.1 mol/l NaOH, and cell-associated radioactivity was determined by liquid scintillation counting.

Cellular apoptosis was measured after overnight treatment of RAW 264.7 macrophages with tryptase (10 ng/ml, Sigma) in the presence or absence of LPA (22 μmol/l, 10 μg/ml). Cells were collected and stained with Annexin V/PI after which the percentage of cell death was measured using flow cytometry.

Microvascular leakage

Microvascular permeability was assessed as previously described (6). In short, male C57Bl/6 mice were injected intradermally at randomized sites with 5×10^5 MC/9 mast cells suspended in PBS containing 50 μg/ml compound 48/80 or 18:1 LPA (10 μg/ml) (n = 6 per group). Immediately after intradermal injection of the cell suspensions, 100 μl 1.25% Evans Blue was injected intravenously and after 30 min the surface area of Evans Blue-stained skin was measured. To measure MC/9 activation in skin, MC/9 cells using the conditions as described above were randomly injected intradermally in mast cell deficient Kit(W^{-sh}/W^{-sh}) mice, which lack endogenous skin mast cells. After 30 min, skin spots were excised and embedded in OCT compound for cryosectioning. Sections 10 μm thick were routinely stained with Alcian Blue/Safranin O (Sigma) and mast cell activation status was scored manually.

Local LPA challenge

Six weeks after collar placement, when advanced atherosclerotic lesions had developed, apoE$^{-/-}$ or apoE$^{-/-}$Kit(W^{-sh}/W^{-sh}) mice were challenged perivascularly by applying pluronic F-127 gel (25% w/v) or pluronic F-127 gel containing LPA (20 μmol/l, ~92 ng/animal) proximal to the collar (n = 8–12 per group). A subset of the LPA-challenged animals received an intravenous injection of the mast cell stabilizer cromolyn (25 mg/kg, Sigma) (6) thirty minutes before and twice daily after local challenge (50 mg/kg ip). Three days after LPA-challenge mice were anesthetized and in situ fixation through the left cardiac ventricle was performed, after which the carotid artery lesions were excised for further analysis.

Histology

Mast cells were visualized by staining of 5 μm cryosections with aqueous Toluidine blue (Sigma). Neutrophils were stained with naphthol AS-D chloroacetate esterase (Sigma). Iron staining was performed according to Perl's method. Monocytes/macrophages were stained immunohistochemically with monocyte/macrophage antibody-2 (MOMA-2) (monoclonal mouse IgG2a, dilution 1:50; Serotec, Kidlington, Oxford, UK). Apoptosis was visualized using a terminal deoxytransferase dUTP nick-end labeling (TUNEL) kit (Roche Diagnostics). Morphometric analysis (Leica QWin image analysis software) was performed on hematoxylin-eosin stained sections of the carotid arteries at the site of maximal stenosis. Toluidine blue-stained sections were used for histological examination for the presence of perivascular mast cells. Neutrophil numbers, mast cell numbers, the extent of mast cell degranulation, and the presence of iron were assessed manually. A mast cell was considered resting when all granula were maintained inside the cell, while mast cells were assessed as activated when granula were deposited in the tissue surrounding the mast cell. MOMA-2 and TUNEL-positive areas were quantified with Leica QWin image analysis software and, in addition, TUNEL-positive nuclei were counted manually. All morphometric analyses were performed by blinded independent operators.

Statistical analysis

Data are expressed as mean ± SEM. A two-tailed Student's *t*-test was used to compare individual groups. Non-Gaussian distributed data were analyzed using a Mann-Whitney U test. Frequency data analysis was performed by means of the Fisher's exact test. A level of $P < 0.05$ was considered significant.

RESULTS

MS imaging

We have applied imaging mass spectrometry via TOF-SIMS for verification and high-resolution spatial localization of lipids in carotid artery lesions from LDLr$^{-/-}$ mice. SIMS analysis shows strong signals for inorganic ions and ionized organic compounds derived from fragmentation of surface molecules. A number of LPA species could be detected in plaque material, and were tentatively assigned on the basis of their M+ peak (**Fig. 1A**). Flanking sections were stained for hematoxylin-eosin and macrophage content (Fig. 1B, C) to correlate intraplaque lipid distribution profiles to morphological features. Color intensity of the ion micrographs corresponded to signal strength (Fig. 1D). Assessment of the intraplaque distribution of these lipids was performed on the basis of their intact mass anions [M-H]$^-$, as determined by LC/MS of crude plaque lipid pools: 14:0 LPA (*m/z* 381), 16:0 LPA (*m/z* 409), 16:1 LPA (*m/z* 407), 18:0 LPA (*m/z* 437), 18:1 LPA (*m/z* 435), 18:2 LPA (*m/z* 433), 18:3 LPA (*m/z* 431), 20:2 LPA (*m/z* 459), 20:3 LPA (*m/z* 457), 22:4 LPA (*m/z* 481), and 22:5 LPA (*m/z* 479). We were able to detect not only LPA isoforms 16:0, 16:1, 18:0, 18:1, 18:2 and 18:3, but also 20:2, 20:3, 22:4, and 22:5 in the atherosclerotic plaque. The individual LPA species show a similar distribution pattern as cholesterol, phosphatidic acids, and triglycerides (Fig. 1E, F), with the most pronounced accumulation in the noncellular core region of the plaque. Thus LPA species,

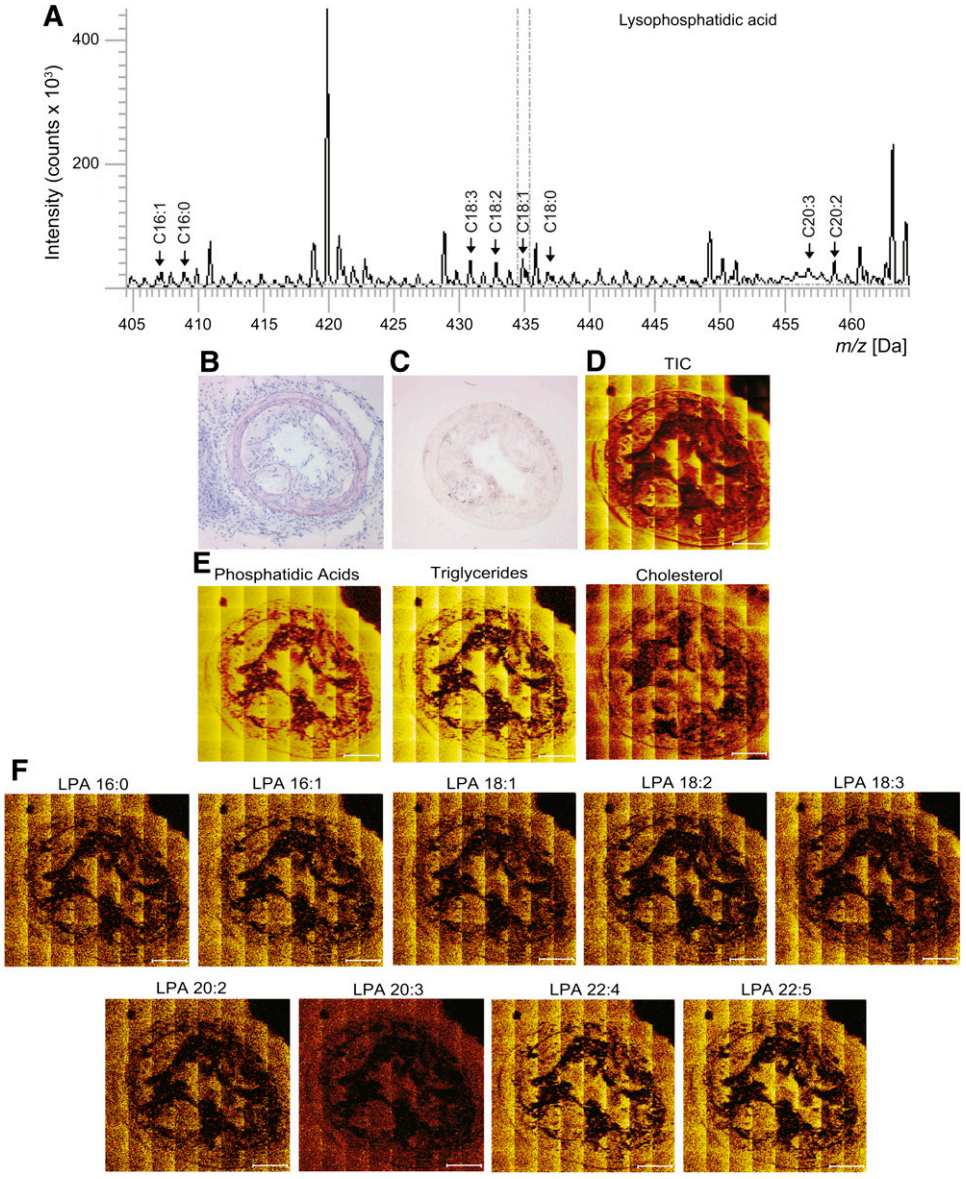

Fig. 1. A: TOF-SIMS spectra recorded from an atherosclerotic artery segment in negative mode with tentative peak assignments, showing LPA species. B: HE staining and C: MOMA-2^{+} macrophage staining of a mouse carotid artery lesion. Negative ion micrographs of a flanking lesion analyzed by TOF-SIMS. Color intensity corresponds to signal strength. D: Total ion current (TIC). E: Intraplaque distribution patterns of a selection of relevant ions including phosphatidic acids, triglycerides, and cholesterol. F: Several LPA species. Scale bar indicates 100 μm.

including 18:1, the biologically most potent isoform and one of the most abundant LPA species (21) (supplementary Fig. I), are abundantly present in the atherosclerotic plaque, in particular in the necrotic core. The LPA assigned peaks detected in SIMS imaging analysis of plaque lysates are identical to *m/z* values obtained by LC/MS spectroscopy, thus providing an orthogonal validation of the SIMS results. Further analysis of the identified LPA peaks using the database provided by the group of Brunelle (27) shows a lack of overlap of the most typical fragments with DAG-H_2O and free fatty acid peaks, making it unlikely that the former result from phospholipid fragmentation.

Mast cell releasate

To determine whether LPA has the capacity to activate mast cells, releasates of compound 48/80 and LPA stimulated MC/9 cells, BMMCs, and freshly isolated peritoneal mast cells were analyzed. Supernatants of untreated mast cells were used as negative controls (0% release), while cell lysates of untreated cells were used for total mast cell content analysis (100%). Both compound 48/80 and LPA were able to induce release of β-hexosaminidase activity and tryptase from MC/9 cells. β-Hexosaminidase activity in the releasate of compound 48/80 and LPA stimulated MC/9 cells did not differ (3.1 ± 0.8% vs. 5.7 ± 1.5% of total release, respectively). Interestingly, tryptase release was much

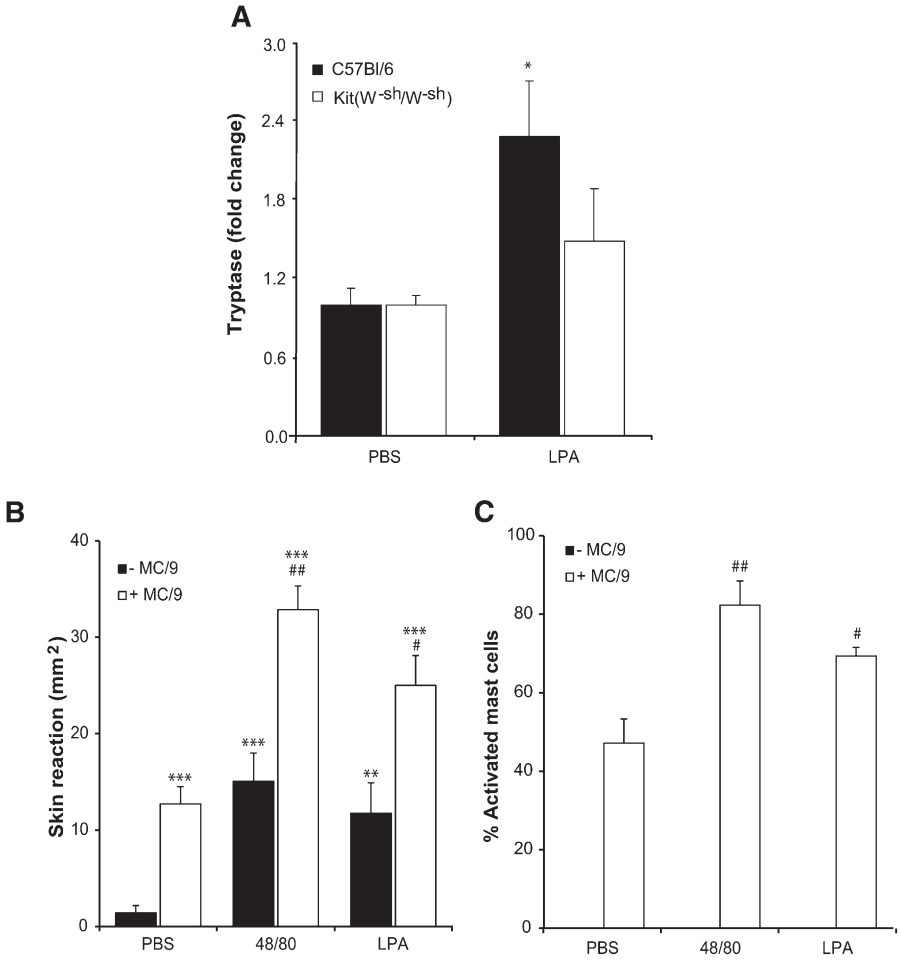

Fig. 2. LPA induces tryptase release from mast cells and induces vascular leakage. A: After intraperitoneal LPA challenge tryptase activity was increased by 2.3-fold in the C57Bl/6 mice, which did not occur in mast cell deficient Kit(W^{-sh}/W^{-sh}) mice. $^{*}P < 0.05$ compared with C57Bl/6 at baseline. B: LPA, compound 48/80, and nonactivated MC/9 cells induced minor to moderate vascular leakage as judged by Evans Blue spot size, probably due to activation of locally residing mast cells. LPA-activated MC/9 cells significantly induced vascular leakage, similarly as compound 48/80-activated MC/9 cells, which were used as positive control. $^{**}P < 0.01$, $^{***}P < 0.001$ compared with PBS control, $^{\#}P < 0.05$, $^{\#\#}P < 0.01$ compared with MC/9. C: Quantification of activated MC/9 cells in skins of mast cell deficient Kit(W^{-sh}/W^{-sh}) mice, illustrating the mast cell absence in PBS, compound 48/80, and LPA injected skins. Injection of unstimulated MC/9 cells resulted in spontaneous activation of 47 ± 6% possibly due to shear stress, a number that was significantly increased by prior mast cell priming with compound 48/80 and LPA. $^{\#}P < 0.05$, $^{\#\#}P < 0.01$ compared with unstimulated MC/9 cells.

higher after LPA stimulation (4.7 ± 1.0% of the total pool was released vs. undetectable levels for compound 48/80). In line with these data, LPA induced β-hexosaminidase activity (9 ± 1%) as well as tryptase activity (6 ± 1%) in the releasate of BMMCs. The LPA_1 receptor antagonist Ki16245 inhibited β-hexosaminidase and tryptase release from MC/9 cells and BMMCs (supplementary Fig. IIA, B), suggesting that LPA mediates mast cell activation mainly via LPA_1. LPA was also seen to induce MCP-1 release from MC/9 cells (46 ± 6 pg/ml, supplementary Fig. IIC), which was at least partly inhibitable by Ki16245 (17 ± 10 pg/ml, $P < 0.05$ compared with LPA). Interestingly, compound 48/80 did not induce MCP-1 release, suggesting that this effect is LPA-specific.

The involvement of LPA_1 in LPA-mediated mast cell activation was further confirmed by our PCR data, establishing that LPA_1 was the main LPA receptor expressed by our murine mast cell cultures (supplementary Fig. III), while LPA_2 and LPA_3 were undetectable. LPA_1 expression was highest in BMMCs that were skewed toward a connective tissue type mast cell, the predominant phenotype in the vessel wall (6).

In peritoneal mast cells, LPA induced β-hexosaminidase activity (7.0 ± 1.2% as compared with 9.1 ± 3.6% for 48/80). LPA again robustly increased tryptase release (19.3 ± 7.0% of total release), while compound 48/80 had only marginal effects (3.0 ± 0.3% of total release). In line with these data, after intraperitoneal LPA challenge tryptase activity in the supernatant was increased by 2.3-fold in C57Bl/6 but not in mast cell-deficient Kit(W^{-sh}/W^{-sh}) mice ($P < 0.05$, **Fig. 2A**). While we did not observe significant differences in the activity of chymase [PBS: 1.0 ± 0.04 vs. LPA: 1.00 ± 0.04

in C57Bl/6 mice; PBS: 1.0 ± 0.12 vs. LPA: 1.08 ± 0.14 in Kit(W^{-sh}/W^{-sh}) mice] and that of β-hexosaminidase [PBS: 1.0 ± 0.05 vs. LPA: 1.25 ± 0.15 in C57Bl/6 mice; PBS: 1.0 ± 0.55 vs. LPA: 0.99 ± 0.16 in Kit(W^{-sh}/W^{-sh}) mice], all displayed as fold change compared with PBS. Taken together, these data demonstrate that LPA is a potent inducer of LPA_1-dependent mast cell activation, and in particular of tryptase and MCP-1 release.

Microvascular leakage in vivo

Mast cells are potent inducers of vascular leakage, which induces plaque destabilization as shown previously (6). To determine whether LPA-mediated mast cell activation enhances vascular leakage, we injected LPA and LPA-activated mast cells intradermally and quantified leakage with Evans Blue dye. LPA and compound 48/80 per se were already seen to induce vascular leakage (Fig. 2B, $P < 0.05$ and $P < 0.001$, respectively), due to activation of resident dermal mast cells as demonstrated previously (6). MC/9 cells without stimulus also induced vascular leakage, possibly due to shear stress-induced activation during injection. We observed that intradermal injection of LPA-activated MC/9 cells highly and significantly induced vascular leakage ($P < 0.001$ compared with PBS control, $P < 0.05$ compared with MC/9 only, Fig. 2B) similarly as the positive control, compound 48/80 activated mast cells ($P < 0.001$ compared with PBS). Intradermal MC/9 injection in mast cell deficient Kit(W^{-sh}/W^{-sh}) mice unequivocally showed that compound 48/80 and LPA induced massive and persistent activation of transferred mast cells in skin (Fig. 2C, $P < 0.01$ and $P < 0.05$, respectively, compared with unstimulated MC/9 cells). These data further establish that LPA is a potent mast cell activator which may affect atherosclerotic plaque stability in vivo.

Local LPA treatment and plaque morphology

We and others have previously demonstrated that LPA progressively accumulates in plaques during disease progression (20, 21) and we here confirmed the presence and actual location of a range of LPA species in the atherosclerotic plaque. We have also firmly established that LPA is a potent mast cell activator. To assess a functional role of LPA in adventitial mast cell activity and plaque progression in vivo, LPA (18:1) was applied perivascularly through a pluronic F-127 gel at the collar-induced carotid artery lesion in $apoE^{-/-}$ mice. As expected, morphometric analysis of the carotid lesions 3 days after challenge did not reveal any differences in plaque size between control and LPA-challenged animals ($92 \pm 13 \times 10^3$ μm^2 vs. $96 \pm 110 \times 10^3$ μm^2 respectively, **Fig. 3A**). Treatment with the mast cell stabilizer cromolyn for 3 days did not affect plaque size as well ($93 \pm 10 \times 10^3$ μm^2). Additionally, no differences were found in medial surface area and percentage of artery stenosis (data not shown).

The number of adventitial mast cells as determined by toluidine blue staining did not differ between LPA- and mock-challenged mice (Fig. 3B), but the percentage of degranulated perivascular mast cells was still increased at time of sacrifice (three days after LPA stimulation, 53 ± 6% vs. 36 ± 7% activated mast cells in control animals, $P = 0.04$, Fig. 3C). As mast cell activation occurs very acutely after application of a stimulus, it is expected that mast cell activation was even further increased earlier after application of LPA. Cromolyn treatment prevented the LPA-induced mast cell activation (38 ± 8% activated mast cells). Perivascular and intimal neutrophil numbers were unaltered after LPA challenge (data not shown). Interestingly, plaque macrophage content was seen to be enhanced upon LPA treatment (15.8 ± 2.7% vs. 9.6 ± 2.0% in control animals, $P < 0.05$, **Fig. 4A**), and this effect did not occur in cromolyn-treated mice (7.2 ± 1.3%, $P < 0.01$ vs. LPA) suggesting that the macrophage accumulation at least in part resulted from mast cell activation. This may possibly be caused by the LPA-mediated release of MCP-1 as shown in vitro. Furthermore, as LPA has been reported to promote macrophage survival (28), we examined the direct effect of LPA on a murine macrophage cell line. We show here that LPA induced a dose-dependent proliferative response in RAW 264.7 murine macrophages (Fig. 4B). No differences were seen with respect to elastic lamina breaks between

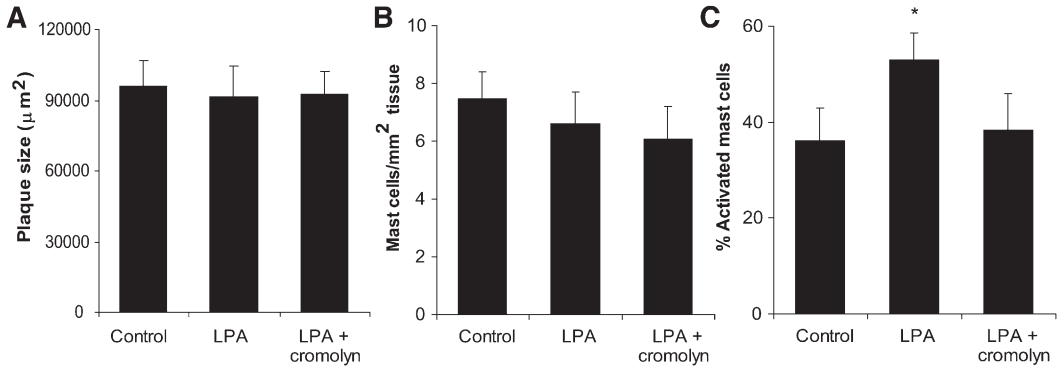

Fig. 3. Adventitial mast cell content of atherosclerotic carotid artery lesions after focal LPA administration. A: Plaque size is not changed at three days after local LPA challenge as compared with control mice or mice that had received the mast cell stabilizer cromolyn. B: Total adventitial mast cell contents of control, LPA-treated, and LPA/cromolyn-treated mice were essentially similar. C: Adventitial mast cell degranulation was increased at three days after local LPA challenge as compared with control mice (*$P < 0.05$). Cromolyn treatment normalized the levels of mast cell activation in the LPA-challenged animals.

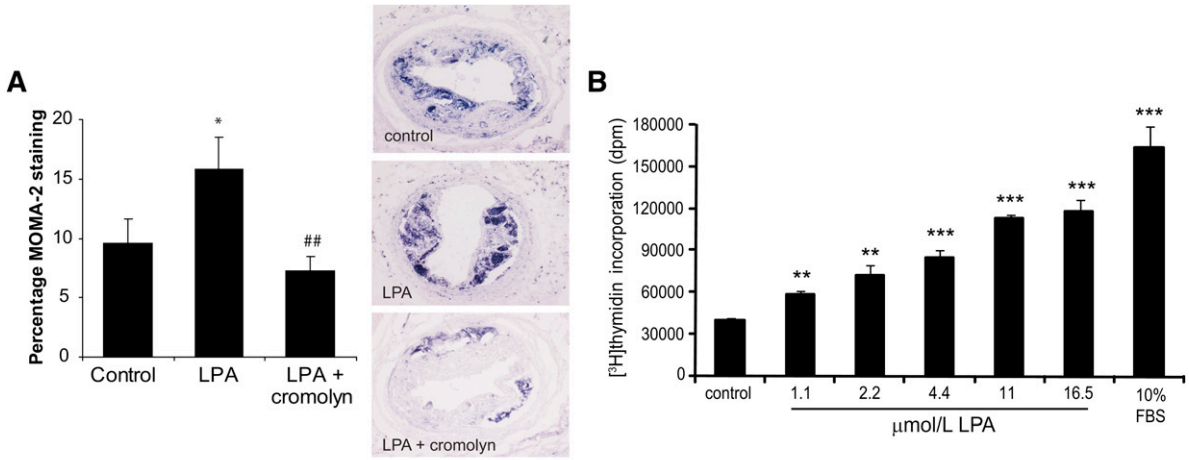

C

Treatment	IPH		Total
	+	-	
control	4	16	20
LPA	10	13	23
LPA + cromolyn	3	12	15

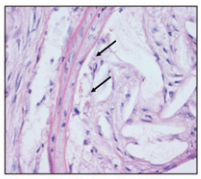

D

Treatment	Iron		Total
	+	-	
control	2	18	20
LPA	7	15	23
LPA + cromolyn	3	12	15

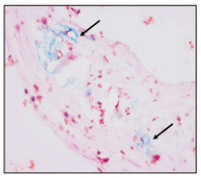

Fig. 4. Effects of LPA on macrophages and hemorrhage. A: Intimal macrophage content in control, LPA-treated, and LPA/cromolyn-treated animals. Intimal macrophage content significantly increased in the LPA-treated group, an effect that was prevented by cromolyn treatment. The right panels are representative MOMA-2 stained cryosections of control (upper panel), LPA-treated (middle panel), and LPA/cromolyn-treated animals (lower panel); $^{*}P < 0.05$ compared to control; $^{\#\#}P < 0.01$ compared to LPA. B: Effect of LPA on murine RAW 264.7 proliferation. A dose-dependent increase in proliferation is seen in RAW 264.7 murine macrophages. $^{**}P < 0.01$, $^{***}P < 0.001$ versus untreated cells (control). C: Quantification of the number of plaques containing intraplaque hemorrhages in control, LPA-treated, and LPA/cromolyn-treated animals suggesting an increased frequency of hemorrhages after LPA challenge. Cromolyn treatment normalized the increase in intraplaque hemorrhage in LPA-challenged animals. A representative hematoxylin/eosin stained cryosection of a plaque from an LPA-challenged mouse is displayed on the right demonstrating intraplaque hemorrhages and erythrocyte extravasation (arrows) in the intima. D: Quantification of the number of Perl's iron positive plaques in control, LPA-treated, and LPA/cromolyn-treated animals suggesting an increased frequency of iron deposits after LPA treatment. Cromolyn treatment normalized the frequency of plaques with iron deposits. On the right is a representative Perl's iron staining revealing large areas with iron deposits (arrows).

groups (LPA: 2.1 ± 0.6 vs. 1.8 ± 0.5 in control animals and 1.4 ± 0.3 in LPA/cromolyn animals). Adventitial and in vitro mast cell degranulation was previously reported to promote apoptosis of vascular smooth muscle cells, endothelial cells, and macrophages (6, 29). TUNEL staining, however, did not reveal any differences in the rate of intimal apoptosis three days after LPA challenge (1.5 ± 0.4% TUNEL positive nuclei vs. 1.2 ± 0.3% in the controls and 2.2 ± 0.6% in LPA/cromolyn animals). In addition, necrotic core size did not differ between the groups (data not shown). In vitro, LPA was not able to rescue macrophages from tryptase-induced apoptosis, suggesting that mast cell-induced apoptosis was compensated for by de novo influx of leukocytes, and possibly mediated by mast cell-derived MCP-1 (supplementary Fig. IV).

Interestingly, LPA-challenged plaques demonstrated the presence of intraplaque hemorrhages characterized by accumulation of intimal erythrocytes in 45% of the plaques in LPA-challenged animals (10 of 23, Fig. 4C), while intraplaque hemorrhage was observed in only 20% of the plaques in control mice (4 of 20, Fig. 4C). The LPA challenge did not enhance the incidence of intraplaque hemorrhage and hemosiderin deposits in lesions in cromolyn-treated mice as these showed comparable numbers to the control group (20%, Fig. 4C). Perl's iron staining confirmed these findings: 7 of 23 (35%) iron positive plaques in the LPA group compared with 2 of 20 (10%) in the control group (Figs. 4D).

To elucidate whether the observed effects of LPA in vivo are mast cell dependent, we challenged mast cell-deficient apoE$^{-/-}$Kit(W^{-sh}/W^{-sh}) mice locally with LPA. LPA challenge did not affect lesion size and any other morphometric parameters in apoE$^{-/-}$Kit(W^{-sh}/W^{-sh}) mice (controls: 125 ± 20 × 10^3 µm^2 vs. LPA: 144 ± 14 × 10^3 µm^2, **Fig. 5A**). We did not observe significant effects on intimal macrophage accumulation between the controls and LPA treated apoE$^{-/-}$Kit(W^{-sh}/W^{-sh}) mice (Fig. 5B). Macrophage content of the apoE$^{-/-}$Kit(W^{-sh}/W^{-sh}) mice was in general lower as compared with apoE$^{-/-}$ mice. Interestingly, LPA did not enhance the incidence of intraplaque hemorrhages in apoE$^{-/-}$Kit(W^{-sh}/W^{-sh}) (0 of 14, $P = 0.01$ compared with LPA treatment in apoE$^{-/-}$ mice, Fig. 5C),

which suggests that LPA induces intraplaque hemorrhage via a mast cell-dependent mechanism.

DISCUSSION

Activated mast cells were shown to accumulate in the arterial adventitia and intima during plaque progression and to promote plaque progression and plaque destabilization (4–6). Oxidized LDL has been proposed as the endogenous stimulus that may be responsible for mast cell activation in atherosclerosis (15, 16). One of oxLDL's main lipid constituents, LPA, has a wide range of effects on mast cells, influencing processes such as proliferation, differentiation, and release of histamine, macrophage inflammatory protein-1β, IL-8, eotaxin, and MCP-1 (18, 19). Moreover, as this bioactive lipid progressively accumulates in plaques during disease progression (20, 21), it may be a likely candidate for vascular mast cell activation in the context of atherosclerosis.

Concordant with our earlier findings, we were able to detect several LPA species in mouse plaques, in particular in the intimal lipid core of the plaque underlying the fibrous cap of the lesion. Our in vitro and in vivo experiments not only confirm that LPA is able to induce mast cell activation but also demonstrate that the secretion pattern after LPA challenge, with preferential release of tryptase over β-hexosaminidase and chymase, differs from that of other stimuli such as compound 48/80, indicating that different activators have different mast cell releasate profiles. In addition, we demonstrate here that LPA-induced mast cell activation enhances microvascular leakage, allowing the influx of detrimental agents and hematopoietic cell subsets such as monocytes and erythrocytes into the atherosclerotic plaque.

One of the features of LPA treatment indeed appeared to be the acute increase in intraplaque hemorrhage incidence, a phenomenon that was also observed after dinitrophenyl hapten-elicited mast cell activation in situ (6). Intraplaque hemorrhage is a potent pro-atherogenic stimulus and risk factor in plaque destabilization, as it is accompanied by deposition of erythrocyte-associated cholesterol and enlargement of the necrotic core of the atherosclerotic plaque. Treatment of mice with cromolyn during LPA challenge, similarly as after dinitrophenyl hapten challenge (6), normalized the extent of mast cell degranulation in the adventitia, while largely preventing intraplaque hemorrhage, implying that mast cells are directly involved in LPA-mediated plaque destabilization.

During the development of atherosclerosis, tissue concentrations of LPA increase (21), thus enhancing local bioavailability of LPA with the capacity to destabilize plaques. Apoptosis at later stages of disease progression is considered deleterious for plaque stability (30). As mast cell degranulation was reported to promote apoptosis of smooth muscle cells (31, 32), endothelial cells (29), and intimal macrophages (6), we established the intimal apoptotic nuclei content after LPA challenge. To our surprise,

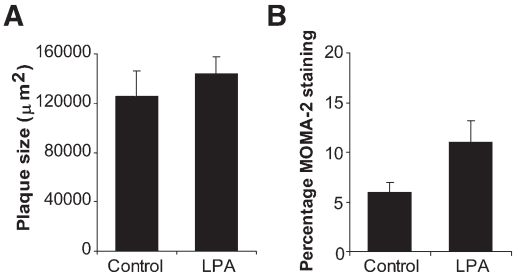

C

Treatment	IPH +	IPH -	Total
control	4	16	20
LPA	10	13	23
LPA (apoE$^{-/-}$/W^{-sh}W^{-sh})	0	14	14 P<0.05

Fig. 5. LPA in mast cell-deficient apoE$^{-/-}$Kit(W^{-sh}/W^{-sh}) mice. A: LPA did not affect lesion size in apoE$^{-/-}$Kit(W^{-sh}/W^{-sh}) mice, while also intimal macrophage content was not significantly changed after LPA challenge (B). C: LPA did not elicit any intraplaque hemorrhages in the mast cell-deficient apoE$^{-/-}$Kit(W^{-sh}/W^{-sh}) mice ($P < 0.05$ as compared with LPA treatment in apoE$^{-/-}$ mice), suggesting that LPA induces intraplaque hemorrhage in a mast cell-dependent fashion.

plaque apoptosis was not altered upon LPA challenge, despite the preferential secretion of tryptase, previously shown by us and others (6, 33) as main culprit in mast cell-associated apoptosis. Possibly the pro-apoptotic effects of the mast cell secretome are counteracted by the intrinsic histone deacetylase and serine threonine kinase (Akt)-dependent anti-apoptotic effects of LPA itself (27, 34). However, in our in vitro studies LPA was not able to rescue macrophages from tryptase induced apoptosis, rendering this theory unlikely. Hypothetically, LPA may also lower the capacity of monocyte-derived cells to emigrate from the vessel wall (35). LPA elicited effects on macrophage content were however completely abolished by cromolyn treatment, which was previously demonstrated to mainly target mast cells without any side effects on other cell types such as neutrophils and macrophages at the dosage used in our animal model (6). It is conceivable that chemotactic effects exerted by LPA-activated mast cells outbalance the aforementioned intrinsic LPA effects. It has already been demonstrated that murine mast cells release a plethora of chemokines including the CXCR2 ligand KC which can trigger directly and indirectly, via very late antigen-4 (36), leukocyte arrest to the endothelium. Furthermore, we now demonstrate that LPA favors mast cell release of MCP-1, which has long since been recognized as one of the primary cytokines in monocyte recruitment to the plaque (37). We thus hypothesize that mast cell degranulation promotes monocyte recruitment, while LPA on its own account will prolong their life span and inhibit their emigration, thereby increasing the plaque macrophage content. Mast cell stabilization by cromolyn possibly reverses this increase by preventing the first step of monocyte recruitment and adhesion.

A few limitations of the study are worth mentioning. First, LPA is a rather heterogeneous class of monoacylated phospholipids that can impact a range of processes besides mast cell function. However, LPA-induced phenotypic

changes in the plaque observed in this study did not occur after treatment with the mast cell stabilizer cromolyn and in mast cell deficient apoE$^{-/-}$Kit(W^{-sh}/W^{-sh}) mice which suggests that in this experimental setup the mast cell is a prominent mediator of the LPA-induced plaque destabilization. Second, the LPA dose used in this study may far exceed endogenously available LPA levels, leading to nonphysiological responses. In previous studies however, we demonstrated that in advanced lesions the level of LPA is approximately 40 pmol/mg atherosclerotic tissue, which corresponds to approximately 35 ng of LPA per plaque. In this study, we locally applied 92 ng of LPA in a pluronic gel that releases its content within three days, which suggests that the dose of LPA used is within a physiological range. Third, in this study we topically applied 18:1 LPA, while in plaque a number of polyunsaturated LPA species were found to accumulate. The latter were shown to display an even higher potency in, for example, platelet activation (38) and this may also hold true for mast cell activation. However, 18:1 LPA is one of the most abundant LPA species in plaque, rendering it highly likely that it is directly accessible for plaque mast cells.

In conclusion, we here provide in vivo proof that LPA bioavailability in the plaque is an important factor in atherosclerotic plaque stability and that effects of LPA are at least partly mediated by LPA-induced mast cell activation. Moreover, we show that enhanced LPA levels in or close to the plaque, as occurring during plaque progression, will increase the plaque macrophage content and induce vascular leakage in a mast cell-dependent manner. LPA has previously been shown to have a number of thrombogenic and atherogenic actions as also recently reviewed by Schober and Siess (39) and these data provide yet another mechanism by which LPA may affect atherosclerotic plaque progression and destabilization. We propose that intervention in LPA bioavailability or activity in the plaque may be an effective measure to reduce mast cell activation and vascular inflammation, improve plaque stability, and concomitantly reduce plaque thrombogenicity, and thus could well represent an effective therapeutic strategy in the prevention of acute coronary syndromes.

REFERENCES

1. Shah, P. K. 2003. Mechanisms of plaque vulnerability and rupture. *J. Am. Coll. Cardiol.* **41:** 15S–22S.
2. Libby, P. 2002. Inflammation in atherosclerosis. *Nature.* **420:** 868–874.
3. Weber, C., A. Zernecke, and P. Libby. 2008. The multifaceted contributions of leukocyte subsets to atherosclerosis: lessons from mouse models. *Nat. Rev. Immunol.* **8:** 802–815.
4. Kaartinen, M., A. Penttilä, and P. T. Kovanen. 1994. Accumulation of activated mast cells in the shoulder region of human coronary atheroma, the predilection site of atheromatous rupture. *Circulation.* **90:** 1669–1678.
5. Laine, P., M. Kaartinen, A. Penttilä, P. Panula, T. Paavonen, and P. T. Kovanen. 1999. Association between myocardial infarction and the mast cells in the adventitia of the infarct-related coronary artery. *Circulation.* **99:** 361–369.
6. Bot, I., S. C. A. de Jager, A. Zernecke, K. A. Lindstedt, T. J. C. van Berkel, C. Weber, and E. A. L. Biessen. 2007. Perivascular mast cells promote atherogenesis and induce plaque destabilization in apolipoprotein E-deficient mice. *Circulation.* **115:** 2516–2525.
7. Sun, J., G. K. Sukhova, P. J. Wolters, L. A. MacFarlane, P. Libby, C. Sun, Y. Zhang, J. Liu, T. L. Ennis, R. Knispel, et al. 2007. Mast cells promote atherosclerosis by releasing proinflammatory cytokines. *Nat. Med.* **13:** 719–724.
8. Healicon, R. M., and J. C. Foreman. 1985. Rat mast cell activation and inactivation: differences when various ligands are used to induce secretion. *Agents Actions.* **16:** 155–159.
9. Bot, I., S. C. de Jager, M. Bot, S. H. van Heiningen, P. de Groot, R. W. Veldhuizen, T. J. van Berkel, J. H. von der Thüsen, and E. A. Biessen. 2010. The neuropeptide substance P mediates adventitial mast cell activation and induces intraplaque hemorrhage in advanced atherosclerosis. *Circ. Res.* **106:** 89–92.
10. Johnson, A. R., T. E. Hugli, and H. J. Müller-Eberhard. 1975. Release of histamine from rat mast cells by the complement peptides C3a and C5a. *Immunology.* **28:** 1067–1080.
11. Wang, J., X. Cheng, M. X. Xiang, M. Alanne-Kinnunen, J. A. Wang, H. Chen, A. He, X. Sun, Y. Lin, T. T. Tang, et al. 2011. IgE stimulates human and mouse arterial cell apoptosis and cytokine expression and promotes atherogenesis in Apoe−/− mice. *J. Clin. Invest.* **121:** 3564–3577.
12. Lappalainen, J., K. A. Lindstedt, R. Oksjoki, and P. T. Kovanen. 2011. OxLDL-IgG immune complexes induce expression and secretion of proatherogenic cytokines by cultured human mast cells. *Atherosclerosis.* **214:** 357–363.
13. Laine, P., A. Naukkarinen, L. Heikkilä, A. Penttilä, and P. T. Kovanen. 2000. Adventitial mast cells connect with sensory nerve fibers in atherosclerotic coronary arteries. *Circulation.* **101:** 1665–1669.
14. Oksjoki, R., P. Laine, S. Helske, P. Vehmaan-Kreula, M. I. Mäyränpää, P. Gasque, P.T. Kovanen, and M. O. Pentikäinen. 2007. Receptors for the anaphylatoxins C3a and C5a are expressed in human atherosclerotic coronary plaques. *Atherosclerosis.* **195:** 90–99.
15. Liao, L., and D. N. Granger. 1996. Role of mast cells in oxidized low-density lipoprotein-induced microvascular dysfunction. *Am. J. Physiol.* **271:** H1795–H1800.
16. Kelley, J., G. Hemontolor, W. Younis, C. Li, G. Krishnaswamy, and D. S. Chi. 2006. Mast cell activation by lipoproteins. *Methods Mol. Biol.* **315:** 341–348.
17. Hashimoto, T., H. Ohata, and K. Honda. 2006. Lysophosphatidic acid induces plasma exudation and histamine release in mice via lysophosphatidic acid receptors. *J. Pharmacol. Sci.* **100:** 82–87.
18. Bagga, S., K. S. Price, D. A. Lin, D. S. Friend, K. F. Austen, and J. A. Boyce. 2004. Lysophosphatidic acid accelerates the development of human mast cells. *Blood.* **104:** 4080–4087.
19. Lin, D. A., and J. A. Boyce. 2005. IL-4 regulates MEK expression required for lysophophatidic acid-mediated chemokine generation by human mast cells. *J. Immunol.* **175:** 5430–5438.
20. Siess, W., K. J. Zangl, M. Essler, M. Bauer, R. Brandl, C. Corrinth, R. Bittman, G. Tigyi, and M. Aepfelbacher. 1999. Lysophosphatidic acid mediates the rapid activation of platelets and endothelial cells by mildly oxidized low density lipoprotein and accumulates in human atherosclerotic lesions. *Proc. Natl. Acad. Sci. USA.* **96:** 6931–6936.
21. Bot, M., I. Bot, R. Lopez-Vales, C. H. van de Lest, J. S. Saulnier-Blache, J. B. Helms, S. David, T. J. C. van Berkel, and E. A. L. Biessen. 2010. Atherosclerotic lesion progression changes lysophosphatidic acid homeostasis to favor its accumulation. *Am. J. Pathol.* **176:** 3073–3084.
22. Cui, M. Z. 2011. Lysophosphatidic acid effects on atherosclerosis and thrombosis. *Clin. Lipidol.* **6:** 413–426.
23. Rizza, C., N. Leitinger, J. Yue, D. J. Fischer, D. A. Wang, P. T. Shih, H. Lee, G. Tigyi, and J. A. Berliner. 1999. Lysophosphatidic acid as a regulator of endothelial/leukocyte interaction. *Lab. Invest.* **79:** 1227–1235.
24. Zhou, Z., P. Subramanian, G. Sevilmis, B. Globke, O. Soehnlein, E. Karshovska, R. Megens, K. Heyll, J. Chun, J. S. Saulnier-Blache, et al. 2011. Lipoprotein-derived lysophosphatidic acid promotes atherosclerosis by releasing CXCL1 from the endothelium. *Cell Metab.* **13:** 592–600.
25. von der Thüsen, J. H., T. J. C. van Berkel, and E. A. L. Biessen. 2001. Induction of rapid atherogenesis by perivascular carotid collar placement in apolipoprotein E-deficient and low-density lipoprotein receptor-deficient mice. *Circulation.* **103:** 1164–1170.
26. Altelaar, A. F., I. Klinkert, K. Jalink, R. P. de Lange, R. A. Adan, R. M. Heeren, and S. R. Piersma. 2006. Gold-enhanced biomolecular surface imaging of cells and tissue by SIMS and MALDI mass spectrometry. *Anal. Chem.* **78:** 734–742.

27. Tahallah, N., A. Brunelle, S. De La Porte, and O. Laprévote. 2008. Lipid mapping in human dystrophic muscle by cluster-time-of-flight secondary ion mass spectrometry imaging. *J. Lipid Res.* **49:** 438–454.
28. Koh, J. S., W. Lieberthal, S. Heydrick, and J. S. Levine. 1998. Lysophosphatidic acid is a major serum noncytokine survival factor for murine macrophages which acts via the phosphatidylinositol 3-kinase signaling pathway. *J. Clin. Invest.* **102:** 716–727.
29. Lâtti, S., M. Leskinen, N. Shiota, Y. Wang, P. T. Kovanen, and K. A. Lindstedt. 2003. Mast cell-mediated apoptosis of endothelial cells in vitro: a paracrine mechanism involving TNF-alpha-mediated down-regulation of bcl-2 expression. *J. Cell. Physiol.* **195:** 130–138.
30. Tabas, I. 2010. Macrophage death and defective inflammation resolution in atherosclerosis. *Nat. Rev. Immunol.* **10:** 36–46.
31. Leskinen, M., Y. Wang, D. Leszczynski, K. A. Lindstedt, and P. T. Kovanen. 2001. Mast cell chymase induces apoptosis of vascular smooth muscle cells. *Arterioscler. Thromb. Vasc. Biol.* **21:** 516–522.
32. den Dekker, W. K., D. Tempel, I. Bot, E. A. L. Biessen, J. A. Joosten, M. G. Netea, J. W. van der Meer, C. Cheng, and H. J. Duckers. 2012. Mast cells induce vascular smooth muscle cell apoptosis via a toll-like receptor 4 activation pathway. *Arterioscler. Thromb. Vasc. Biol.* **32:** 1960–1969.
33. Zhang, J., J. Sun, J. S. Lindholt, G. K. Sukhova, M. Sinnamon, R. L. Stevens, R. Adachi, P. Libby, R. W. Thompson, and G-P. Shi. 2011. Mast cell tryptase deficiency attenuates mouse abdominal aortic aneurysm formation. *Circ. Res.* **108:** 1316–1327.
34. Ishdorj, G., B. A. Graham, X. Hu, J. Chen, J. B. Johnston, X. Fang, and S. B. Gibson. 2008. Lysophosphatidic acid protects cancer cells from histone deacetylase (HDAC) inhibitor-induced apoptosis through activation of HDAC. *J. Biol. Chem.* **283:** 16818–16829.
35. Llodrá, J., V. Angeli, J. Liu, E. Trogan, E. A. Fisher, and G. J. Randolph. 2004. Emigration of monocyte-derived cells from atherosclerotic lesions characterizes regressive, but not progressive, plaques. *Proc. Natl. Acad. Sci. USA.* **101:** 11779–11784.
36. Schramm, R., T. Schaefer, M. D. Menger, and H. Thorlacius. 2002. Acute mast cell-dependent neutrophil recruitment in the skin is mediated by KC and LFA-1: inhibitory mechanisms of dexamethasone. *J. Leukoc. Biol.* **72:** 1122–1132.
37. Boring, L., J. Gosling, M. Cleary, and I. F. Charo. 1998. Decreased lesion formation in CCR2−/− mice reveals a role for chemokines in the initiation of atherosclerosis. *Nature.* **394:** 894–897.
38. Tokumura, A., J. Sinomiya, S. Kishimoto, T. Tanaka, K. Kogure, T. Sugiura, K. Satouchi, K. Waku, and K. Fukuzawa. 2002. Human platelets respond differentially to lysophosphatidic acids having a highly unsaturated fatty acyl group and alkyl ether-linked lysophosphatidic acids. *Biochem. J.* **365:** 617–628.
39. Schober, A., and W. Siess. 2012. Lysophosphatidic acid in atherosclerotic diseases. *Br. J. Pharmacol.* **167:** 465–482.